

Accepted Manuscript

Electromechanical characteristics and numerical simulation of a new smaller magnetorheological fluid damper

Junhui Li , Zhihui Liu , Zhan Liu , Liutian Huang , Can Zhou ,
Xiaohe Liu , Wenhui Zhu

PII: S0093-6413(18)30208-8
DOI: [10.1016/j.mechrescom.2018.07.010](https://doi.org/10.1016/j.mechrescom.2018.07.010)
Reference: MRC 3292



To appear in: *Mechanics Research Communications*

Received date: 12 April 2018
Revised date: 3 July 2018
Accepted date: 30 July 2018

Please cite this article as: Junhui Li , Zhihui Liu , Zhan Liu , Liutian Huang , Can Zhou , Xiaohe Liu , Wenhui Zhu , Electromechanical characteristics and numerical simulation of a new smaller magnetorheological fluid damper, *Mechanics Research Communications* (2018), doi: [10.1016/j.mechrescom.2018.07.010](https://doi.org/10.1016/j.mechrescom.2018.07.010)

This is a PDF file of an unedited manuscript that has been accepted for publication. As a service to our customers we are providing this early version of the manuscript. The manuscript will undergo copyediting, typesetting, and review of the resulting proof before it is published in its final form. Please note that during the production process errors may be discovered which could affect the content, and all legal disclaimers that apply to the journal pertain.

Highlights

- A new MRF damper with outer-coils and testing system was designed. The MRF has good mechanical properties when the damping gap is 1.5mm. The smoothing damping force is only 1.0-4.0N, and it is the linear function with the current. The damping force versus velocity curve has obvious hysteresis characteristic, and an improved nonlinear dynamic model is proposed. The electromechanical characteristics of the MRF damper can be simulated by Simulink, which provides an analysis platform for applications.

ACCEPTED MANUSCRIPT

• **Electromechanical characteristics and numerical simulation of a new smaller magnetorheological fluid damper**

Junhui Li, Zhihui Liu, Zhan Liu, Liutian Huang, Can Zhou*, Xiaohe Liu*, and Wenhui Zhu*

State Key Laboratory of High Performance Complex Manufacturing and School of Mechanical and Electrical Engineering, Central South University, Changsha 410083, China

*Corresponding author: Can Zhou(zhoucan@csu.edu.cn), Xiaohe Liu(liuxh@@csu.edu.cn) and Wenhui Zhu(zhuwenhui@csu.edu.cn)

Abstract—In order to develop a smaller magnetorheological fluid (MRF) damper and its corresponding analysis software, a new MRF damper with outer-coils and testing system was designed. The testing results show that the MRF has good mechanical properties when the damping gap is 1.5mm. The smoothing damping force is only 1.0-4.0N by adjusting the coil current from 0A to 2A, and it is linearly related to current through data fitting. The damping force versus velocity curve has obvious hysteresis characteristic, and an improved nonlinear dynamic model is proposed. Based on the model and linear function, electromechanical characteristics of the MRF damper can be simulated by Simulink, which provides an analysis platform for applications of the damper.

Index Terms—Smaller MRF damper; electromechanical simulink; damping gap; electromechanical characteristics.

I. INTRODUCTION

With the emergence of new intelligent materials and the wide use of semi-active control technology, magnetorheological technology attracts more and more attention of researchers. Magnetorheological fluid (MRF) is mainly composed of soft magnetic particles, mother liquor and additives to prevent the settling of the mixture of particles [1-4]. Under the condition of magnetic field, the MRF can transform from free-flowing liquid to highly viscosity, low-flow Bingham fluid in millisecond time, and the change is continuous and reversible, the yield strength is controllable [5-8]. It is the intelligence and stability, making the MRF has received extensive attention in the field of science and technology in recent years, which to a certain extent promoted the development of the semi-active control [9-12].

Among all the application of using magnetorheological technology, the MRF damper based on magnetorheological effect is a semi-active control device with good performance. It has the advantages of simple structure, fast response, large dynamic range, good durability and strong reliability [13-15]. In reality, MRF dampers are mostly used in heavy machinery, construction, medical, and bridge cables nowadays [16]. For example, the United States Lord Corporation developed a full-scale MRF damper whose output of damping force up to 180kN [17], even the smaller MRF damper such as MR101097, its minimum output of damping force also reached 100N [18]. It is not suitable for some applications where the force needed less than 100N, not to mention of meeting

the soft landing force of less than 10N required for flip chip bonding of microelectronics packaging [19-24]. So, the smaller damping system needs to be developed and the appropriate analysis software needs to be researched for practical application.

Therefore, this study was undertaken to design a smaller MRF damper to obtain the output of damping force of less than 4N. The electromechanical property of MRF damper was tested by the test equipment. Based on the experimental data, the general equation of the output damping force was deduced, and the model was simulated by Simulink.

Design and experiment

1) *Structure Design of the micro MRF damper*

According to the different motion modes of the MRF in damper, MRF damper is generally divided into four types: shear type, valve type, shear valve type and squeeze valve type [25-27]. Because the shear valve type possesses both the advantages of shear type and valve type, its output adjustable damping force has a large range, and the design of magnetic circuit is simple. Therefore, the design of MRF damper adopted shear valve type.

For the miniature damper system, the general inner winding mode cannot be manufactured and assembled, therefore, a novel outer winding type was used in this miniature damper system.

The damping force of the MRF damper consists of two parts: on the one hand, the piston squeezes the MRF on one side of the cylinder to increase the pressure, and the pressure difference is generated in the cavity of the damper, the difference made the MRF flow through the gap of the cylinder piston to the other

side, resulting in extrusion pressure F_V , on the other hand, the relative motion of the cylinder and the piston drags the MRF from one side to another side, a shear force F_S is generated. Therefore, the damping force of the shear valve type MRF damper is the sum of the above two parts, namely:

$$F_{SV} = F_S + F_V \quad (1)$$

According to the Bingham model, the shearing force and extrusion force are calculated as follows:

$$F_V = \frac{12\eta l A_p}{\pi d h^3} A_p v + \frac{3l\tau_y}{h} A_p \quad (2)$$

$$F_S = \frac{\pi\eta DL}{h} v + \pi DL\tau_y \text{sgn}(v) \quad (3)$$

$$F_{SV} = \frac{3\eta l[\pi(D^2 - d^2)]^2}{4\pi d h^3} v + \frac{3l\pi(D^2 - d^2)}{4h} \tau_y \text{sgn}(v) \quad (4)$$

Where η is the equivalent viscosity, A_p is the effective area of the piston, h is the damping gap, v is the rate, and τ_y is the shear yield strength. D is the piston diameter, L is the effective length of the piston, and the sign function $\text{sgn}(v)$ is to consider the reciprocating motion of the piston. According to the above formula, the main parameters affecting the MRF damper are damping clearance h , piston effective length L and piston diameter D . With the increase of the damping gap h , the adjustable multiples of the damper increase, and the damping force decreases. In order to strike a balance between them, we took h in the design of 1-2mm. The larger the piston length L , and the greater the output of damping force, but the increase of L will increase the length of the cylinder, which makes the size of the damper become larger. Taking it into account, took $L=8\text{mm}$. The piston diameter D determines the area of the piston, and increase the area can increase the damping force, but reduce the adjustable coefficient at the same time[28], so D should be appropriate, and took $D=5-7\text{mm}$. In addition, the piston rod as an important part of the transmission force, its strength and stiffness should meet the formula:

$$d \geq \sqrt{\frac{4F}{\pi[\sigma]}} \quad (5)$$

In order to minimize the size of MRF damper as much as possible, and considering the difficulty of processing, we finally took $d=2\text{mm}$.

In terms of the selection of materials, in order to realize the transient response of the MRF damper, the piston rod of the materials should meet the requirements of good magnetic conductivity and quick demagnetization. Early researchers compared silicon steel with carbon steel magnetization curve and found that silicon steel is significantly faster than carbon steel both in the magnetic and demagnetization [29]. Therefore, in order to get the optimal experiment results, silicon steel was chosen as the material of the

piston rod. In order to make as many lines of magnetic force as possible into the cylinder, aluminum alloy with weak magnetization but high mechanical strength was chosen as the material of the cylinder in this study. Likewise, the aluminum alloy was also selected as the end cover material. The whole sealing method adopted the double sealing device with sealing ring and sealing gasket. The main structural parameters of the designed micro MRF damper are shown in TABLE I. The assembled MRF damper is shown as Fig. 1.

TABLE I Main structural parameters of MRF damper

Part	Size (mm)	Material
Piston rod diameter d	2	Silicon Steel
Piston diameter D	5、6、7	Silicon Steel
Piston length L	8	Silicon Steel
Inner diameter of the cylinder	9	Aluminum alloy
Outer diameter of the cylinder	11	Aluminum alloy

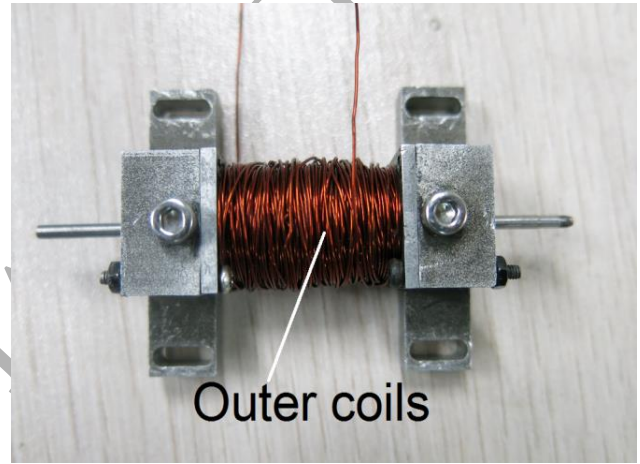


Fig. 1 Picture of the MRF damper

2) Experimental testing platform

After the design of MRF damper is completed, we conducted a series of experiments to test its mechanical properties, observed and analyzed its performance through the experimental data. Therefore, an experiment platform was set up, it mainly including hardware part and software part.

The hardware of the experimental platform mainly includes computer, motion control card, connecting components, the drive, drive motor and motion platform. After platform was set up, the related components must be programmed to run smoothly. Labview software was used to write the motion control program to realize the motion control of the experiment platform. The whole working process of the experimental platform is as follows: The MRF damper was fixed on the screw rod through the connecting components, computer sends the command to motion control card. After receiving the instruction, the signal was processed and servomotor was driven by the control card, driving the MRF damper move to realize

the loading of the force. The force signal was transformed into a voltage signal by a piezoelectric sensor, and then amplified to the data acquisition card via a charge amplifier. At the same time, it was transmitted to the current controller in the form of pulse and was converted into a stable current value, then was transmitted to the coil, achieved the goal of controlling the magnitude of damping force. The whole experimental platform is shown in Fig. 2.

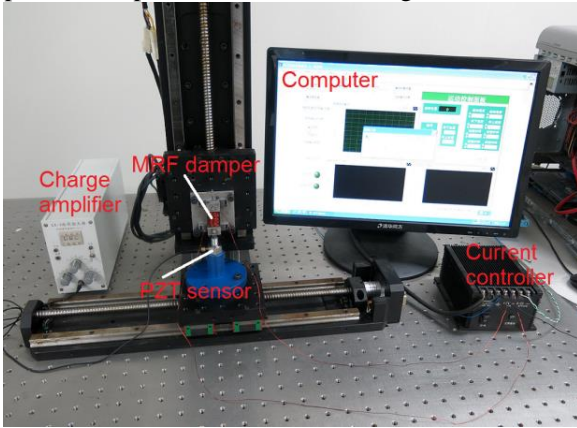


Fig. 2 Experimental platform

II. EXPERIMENT AND RESULT ANALYSIS

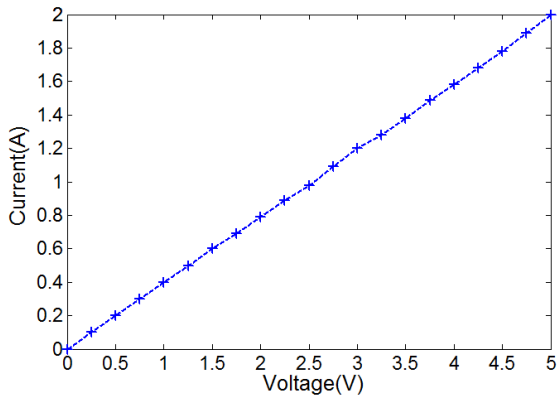


Fig. 3 Current versus voltage curves

From the above analysis, it can be seen that the damping force and damping force adjustable range of MR dampers are two important parameters, and the most significant factor is damping gap. When damping gap increases, damping force reduces, and the adjustable range of damping force is larger. In order to obtain a larger output damping force and a suitable damping force adjustable range, we adopted three different diameter pistons in this experiment, corresponding to the damping gap of 1mm, 1.5mm, 2mm, respectively. After the experimental device was connected, different analog voltage was inputted on the computer to achieve the purpose of supplying the corresponding current to the coil, the correspondence

between the analog voltage and the output current is shown as Fig. 3.

The relationship between the current and voltage is expressed as Equation 6:

$$U = 0.25 \cdot I \quad (6)$$

The different currents of 0-2A were applied to the coils respectively, and the results of the three different damping gaps were obtained in Fig. 4.

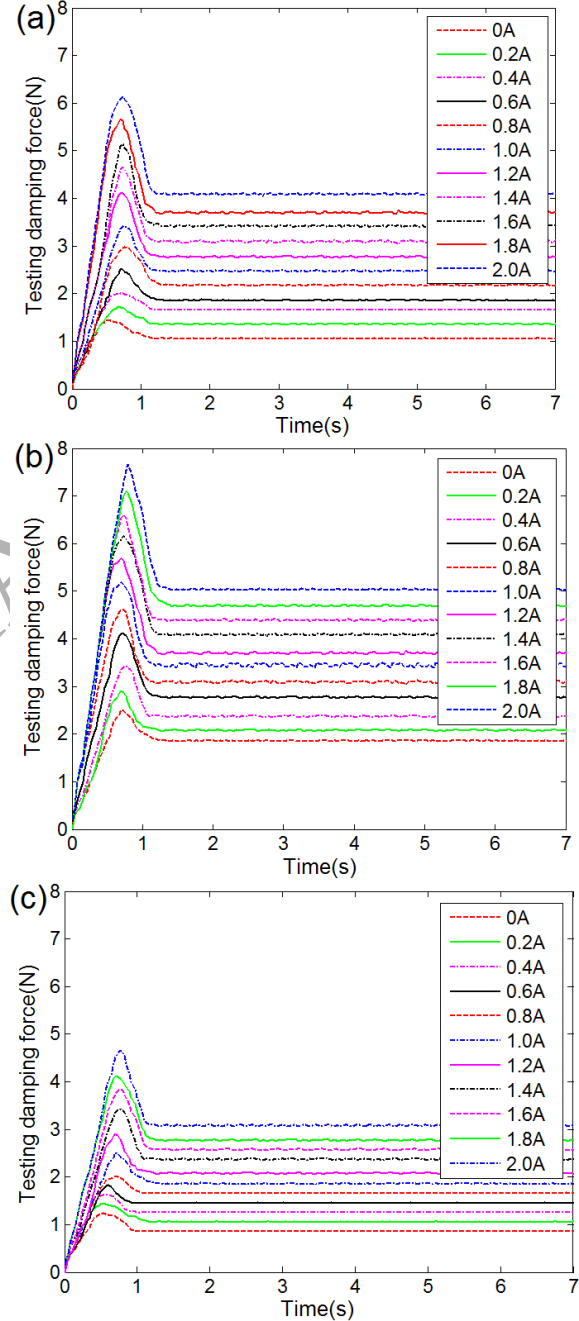


Fig.4 The testing damping force versus time under different currents for 1 mm gap (a) 1.5 mm gap (b) and 2 mm gap (c)

From the Fig. 4, we can see that the experimental results under the three kinds of damping gap show a

similar law: The damping force begins to rise rapidly to a peak value, then descends rapidly and tends to be gentle, finally maintains a relatively stable value. Both the maximum impact force and the smoothing damping force increase with current. Since the data is an average of the repetitions of fifty experiments, the accidental situation was ruled out. In order to compare the adjustable ranges of the three kinds of damping gaps, we put the damping force of the MR dampers with damping gaps of 1 mm, 1.5 mm, and 2 mm on the curve of current in a graph shown as Fig. 5.

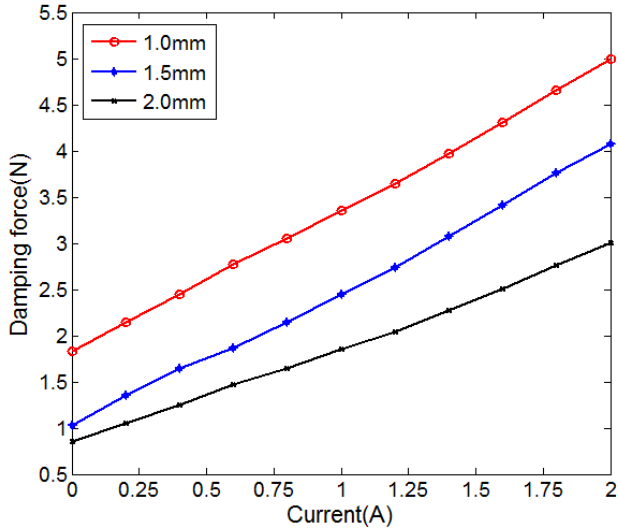


Fig. 5 Curve of force versus current for three damping gap

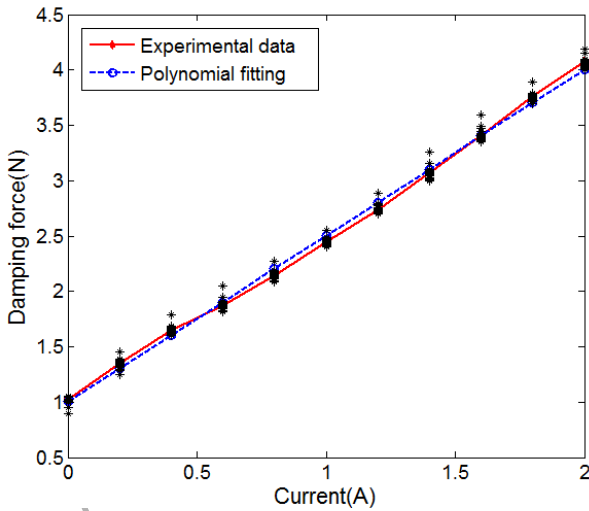


Fig. 6 Damping force versus current curve

The experimental results show that when the damping gap is 1mm, the maximum value of smooth damping force is 5.0N, the minimum value is 1.85N, the adjustable coefficient is $5.0/1.85=2.7$; when the damping gap is 1.5mm, the maximum value of smooth damping force is 4.00N, the minimum value is 1.00N, the adjustable coefficient is $4.00/1.00=4.00$; when the

damping gap is 2mm smooth, the maximum damping force is 3.01N, the minimum value is 0.85N, the adjustable coefficient is $3.01/0.85=3.54$. By comparison, it was found that the MRF damper with damping gap of 1.5mm has the maximum damping force adjustable coefficient, so the MRF damper with 1.5mm damping gap was chosen to further study.

The damping force increases with the increase of the current, and they show a certain positive correlation. In order to explore the quantitative relationship between the damping force and the current, we performed 30 repeated experiments on 1.5mm damping gap MRF damper, the fitting curve and the experimental data are shown respectively in Fig. 6.

The relationship between damping force and current was obtained by polynomial fitting:

$$F = 1.5x + 1.004 \quad (7)$$

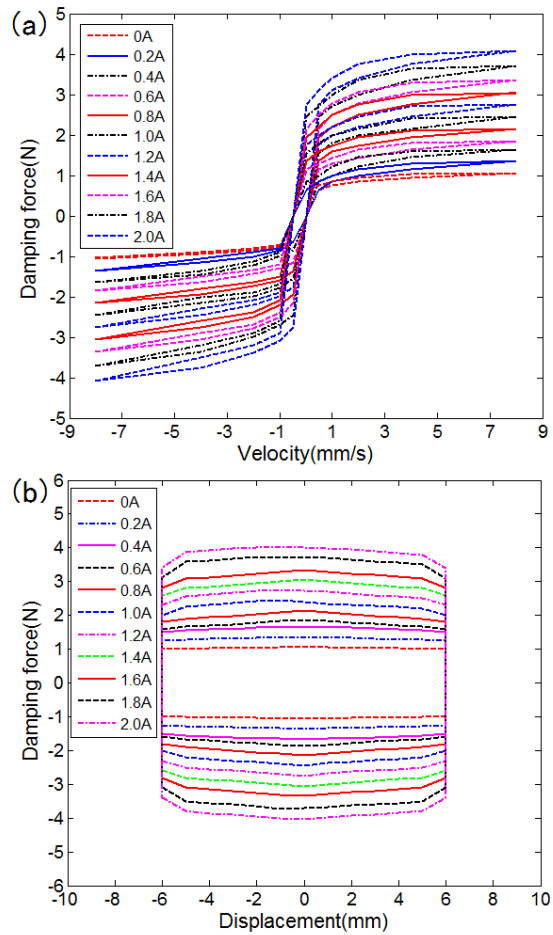


Fig.7 curves of damping force versus velocity under different currents (a) and damping force and displacement under different currents (b)

Through the mathematical analysis, the fitting curve and the actual numerical variance SSE is only 0.02507, the mean square error RMSE is only 0.05278, and the determination coefficient R-Square is 0.9975. The results show that the fitting effect is good and the error

is within the allowable range. This formula can accurately describe the relationship between the damping force and current. In order to further study the relationship between the damping force versus the velocity and displacement, we adopted the same test method to apply different currents to the MRF damper. The input currents are 0A, 0.2A, 0.4A, 0.6A, 0.8A, 1.0A, 1.2A, 1.4A, 1.6A, 1.8A and 2.0A, respectively. The mechanical properties under different input currents were tested. The test experimental results are shown in Fig. 7.

The experimental results show that, under the same frequency, the magnitude of damping force is related to the input current and speed. The larger the input current and velocity are, the larger the damping force is, and the damping force versus velocity curve has obvious hysteretic characteristics. The larger the input current, the more obvious the hysteresis characteristic.

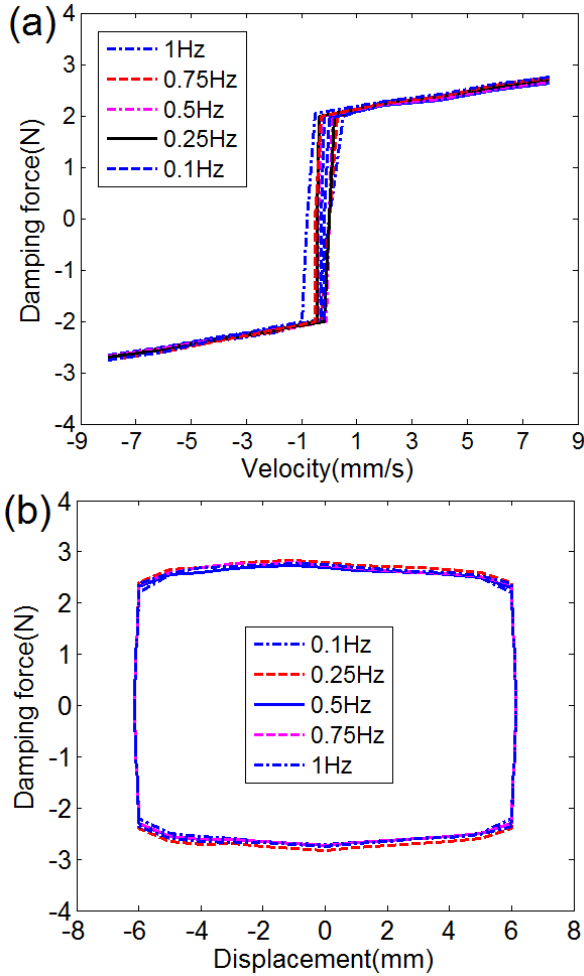


Fig. 8 curves of damping force versus velocity at different frequencies (a) and damping force versus displacement at different frequencies (b)

In the same way, the MRF damper was applied with different frequencies, the testing frequency was set to

0.1Hz, 0.25Hz, 0.5Hz, 0.75Hz and 1.0Hz, respectively. The experimental results are shown in Fig. 8.

The results show that the damping force is almost independent with the excitation frequency under the same input current. The relationship between the damping force and the displacement changes very little with the change of frequency. However, at different frequencies, the damping force and velocity relationship curve still exists hysteresis characteristics, the greater the excitation frequency, the more obvious the hysteresis characteristics.

III. SIMULINK PLATFORM CREATION

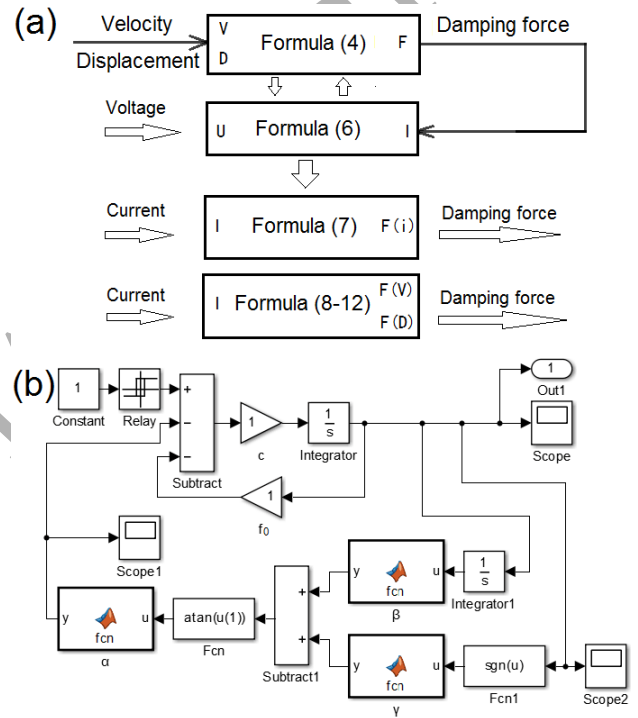


Fig. 9 The diagram of the simulation model from (a) and simulation program block diagram from (b)

Based on the experimental results of the MRF damper, and through the theoretical derivation, an improved nonlinear dynamic model was proposed, the expression of which is shown as equation 8.

$$F = c\dot{x} + \alpha \tan^{-1}(\beta\dot{x} + \delta \text{sgn}(\dot{x})) + f_0 \quad (8)$$

Where c is the viscous damping coefficient, x is the displacement of the piston, \dot{x} is the speed of the piston, f_0 is a biasing force, α , β , and δ are undetermined parameters associated with hysteresis characteristics. These parameters vary with the input current. According to the experimental data of the test, the relationship between each parameter and input current is obtained by data processing. The model parameter identification is carried out respectively by Matlab

program with genetic algorithm based on the test results of different frequencies, different amplitudes, and different currents. And the regression fitting was carried out. Each of the four parameters can be obtained by the polynomial fitting shown as follows,

$$c = 0.01i^3 + 0.03i^2 - 0.03i + 0.18 \quad (9)$$

$$\alpha = -0.52i^3 + 2.75i^2 - 3.31i + 3.82 \quad (10)$$

$$\beta = 490.74i^2 - 894.25i + 508.16 \quad (11)$$

$$\delta = 45.86i^2 - 8.32i + 59.67 \quad (12)$$

Where i is the input current.

In order to validate the model and develop an analysis software of MRF damper, we use Simulink to create a platform for the above model, the diagram of the simulation model is shown in Fig. 9.

To verify its validity, an arbitrary current is entered. When the current is input, easy to get the damping force, the current and damping force simulation curve is shown as Fig. 10. For example, when we enter $i=1.2A$, run the program, which will show the velocity and displacement simulation curves, as shown in Figure 10.

It can be seen from the comparison that the simulation results are in good agreement with the experimental curves, which shows that the Simulink module can describe the electromechanical properties of the micro MRF damper very well. As long as the input current value is changed, the damping force and the simulation curve can be obtained under different conditions. Therefore, a GUI interface in MATLAB based on the simulation module was designed, and an analysis software of MRF damper was obtained.

IV. CONCLUSION

The novel outer coil mode was confirmed, promoting the development of the smaller MRF damper. The MRF damper with 1.5mm damping gap has good electromechanical properties. In this paper, by reducing the size of the MRF damper, the smoothing damping force was reduced to 1N-4N. It was found that the damping force has a linear relationship with the current, and this relation can be expressed by primary curve. The damping force shows obvious hysteresis with the increase of velocity, this phenomenon is becoming more and more significant with the increase of current and frequency. There is no obvious relationship between damping force and frequency, frequency has little effect on the damping force-displacement curve. The damping force of the MRF damper can be expressed by a nonlinear dynamic model. Simulink simulations show that the model is in good agreement with the experimental curves. For this

reason, an analysis software was developed to promote the MR theory and technology improvement.

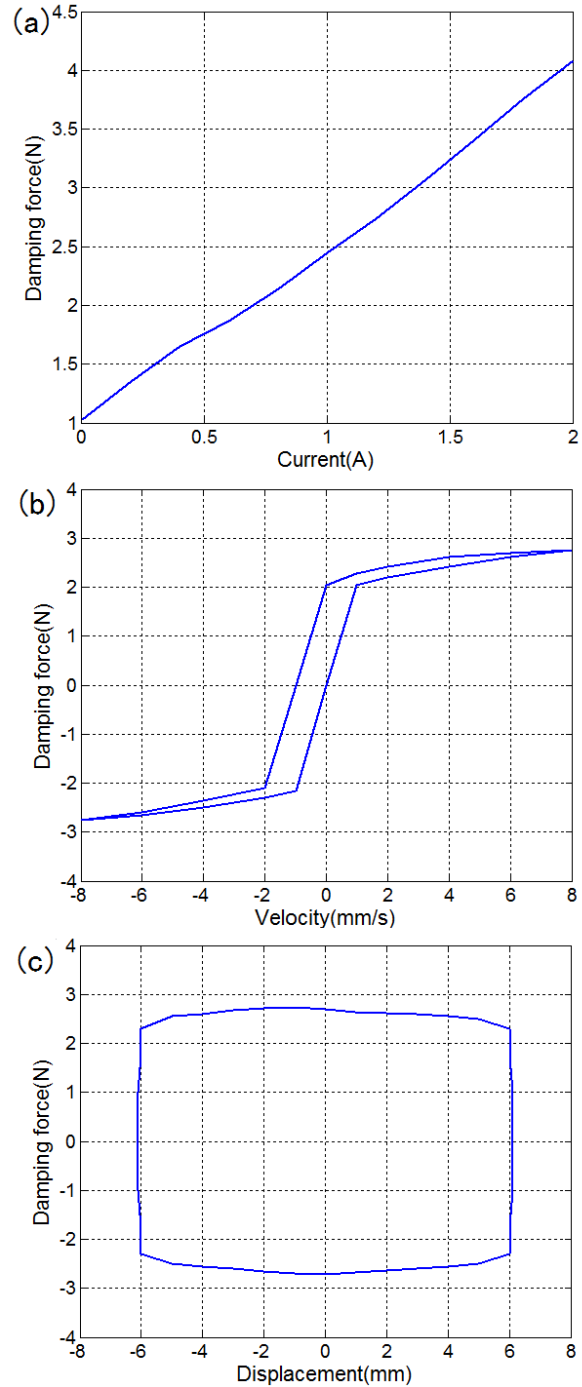


Fig.10 Current-damping force simulation curve (a) and Velocity-damping force simulation curve (b) and Displacement - damping force simulation curve (c)

REFERENCES

- [1] H. S. Kang, J. P. Bong, J. C. Young, "Effect of magnetic nano particle additive on characteristics of magnetorheological fluid", *IEEE Trans. Magn.*, vol.45, no.10, pp.4045-4048, 2009.
- [2] T. L. Sung, S. C. Min, "Magnetorheological characterization of

- carbonyl iron based suspension stabilized by fumed silica”, *J. Magn. Mater.*, vol.282, no.1, pp.170-173, 2004.
- [3] J. Zeng, Y. Guo, J. Zhu, “Investigation and Simulation on Magnetic Hysteresis Properties of Magnetorheological Fluid”, *IEEE Trans. Ind. Electron.*, vol.64, no.2, pp.1611-1616, 2017.
- [4] X. Tang, H. Du, S. Sun, D. Ning, Z. Xing, W. Li, “Takagi–Sugeno Fuzzy Control for Semi-Active Vehicle Suspension With a Magnetorheological Damper and Experimental Validation,” *IEEE-ASME Trans. Mech.*, Vol.22, no.1, pp. 291-300, 2017.
- [5] S. J. Dyke, B. F. Spencer, M. K. Sain, “Modeling and control of magnetorheological dampers for seismic response reduction”, *Smart Mat. Struct.*, vol.5, no.5, pp.565-575, 1995.
- [6] R. Maheshwari, S. Munk-Nielsen, K. Lu, “An active damping technique for small dc-link capacitor based drive system”, *IEEE Trans. Ind. Inform.*, vol. 9, no. 2, pp 848-858, 2013.
- [7] L. Du, T. Shi, L. Su, D. Xue and G. Liao, “A novel bottom–up copper filling of blind silicon vias in 3D electronic packaging”, *Micromech. Microeng.*, 25045005, 2015.
- [8] G. A. Dominguez, M. Kamezaki, S. Sugano, “Proposal and Preliminary Feasibility Study of a Novel Toroidal Magnetorheological Piston,” *IEEE-ASME Trans. Mech.*, 2016. DOI: 10.1109/TMECH.2016.2622287
- [9] C. Spelta et al, “Control of magneto-rheological dampers for vibration in a washing machine Mechatronic”, *Mech.*, vol.19, no.3, pp.410–421, 2009.
- [10] D. Case, B. Taheri, and E. Richer, “Design and Characterization of a Small-Scale Magnetorheological Damper for Tremor Suppression,” *IEEE-ASME Trans. Mech.*, vol.18, no.1, pp 96-103, 2013.
- [11] A. Milecki, “Investigation and control of magnetorheological fluid dampers”, *Int. J. Mach. Tools Manuf.*, vol.41, no.1, pp.379-391, 2004.
- [12] L. Yu, L. Ma, J. Song, X. Liu, “Magnetorheological and Wedge Mechanism-Based Brake-by-Wire System With Self-Energizing and Self-Powered Capability by Brake Energy Harvesting,” *IEEE-ASME Trans. Mech.*, Vol.21, no.5, pp. 2568-2580, 2016.
- [13] V. García, P. Catalágregori, J. Madrid, “Semiactive Vibration Control of a Smart Seat with an MR Fluid Damper Considering its Time Delay”, *J. Inter. Mat. Syst. Str.*, vol.13, no.7-8, pp.521-524, 2002.
- [14] J. Li, L. Han, J. Duan and J. Zhong, “Interface mechanism of ultrasonic flip chip bonding”, *Appl. Phys. Lett.* vol.90, no.24, pp.2902-2903, 2004.
- [15] Y. Q. Ni, Y. Chen, J. M. Ko, “Neurocontrol of cable vibration using semi-active magnetorheological dampers”, *Eng. Struct.*, vol.24, no. 2, pp.295-307, 2004.
- [16] J. D. Caslon, K. D. Weiss, “A growing attraction to magnetic fluids”, *Mac. Des.*, vol.66, no.15, pp.61-64, 1994.
- [17] G. Q. Yang, J. Spencer, F. Billie, “Dynamic modeling of large-scale magnetorheological damper systems for civil engineering applications”, *J. Eng. Mech-Asce.*, vol.130, no.9, pp.1107-1114, 2004.
- [18] Z. Li, Y. Lv, L. Xu, “Experimental studies on nonlinear seismic control of a steel concrete hybrid structure using MR dampers”, *Eng.Struct.*, vol.49, no.4, pp. 248-263, 2013.
- [19] F. L. Wang, L. Han, J. Zhong, “Effect of ultrasonic power on the heavy aluminum wedge bonding strength”, *J. Mech. Eng.*, vol.18, no.4, pp.515-518, 2005.
- [20] C. Zhou, J. Duan, G. Deng, and J. Li, “ A novel high speed jet dispenser driven by double piezoelectric stacks”, *IEEE Trans. Ind. Electron.*, vol.64, no.1, pp:412-419, 2017.
- [21] H. Xu, I. Qin, H. Clauberg, B. Chylak, and V.L. Acoff, “Behavior of palladium and its impact on intermetallic growth in palladium-coated Cu wire bonding”, *Acta Mater.*, vol.61, no.1, pp. 79-88, 2013.
- [22] Junhui Li, Xiaorui Zhang, Can Zhou, Jingan Zheng, Dasong Ge, and Wenhui Zhu, New applications of an automated system for high-power LEDs, *IEEE-ASME Trans. Mech.*, 2016, 21(2):1035-1042.
- [23] Can Zhou, Junhui Li, Ji’an Duan, Guiling Deng, Control and jetting characteristics of an innovative jet valve with zoom mechanism and opening electromagnetic drive, *IEEE-ASME Trans. Mech.*, 2016, 21(2):1185-1188.
- [24] J. Li, W. Tian, H. Liao, C. Zhou, X. Liu, W. Zhu, The mathematical model & novel final test system for wafer-level packaging, *IEEE Trans. Ind. Inform.*, 2017, DOI: 10.1109/TII.2016.2643694.
- [25] L. Du, T. Shi, P. Chen, L. Su, J. Shen, J. Shao and G. Liao, “Optimization of through silicon via for three-dimensional integration”, *Microe. Eng.*, vol.139, no.1, pp. 31–38, 2015.
- [26] N. M. Wereley, L. Pang and G. M. Kamath, “Idealized hysteresis modeling of electrorheological and magnetorheological dampers”, *J. Intell. Mater. Syst. Struct.* vol.9, no.8, pp.642-649, 1998.
- [27] K. J. Li, G. Y. Tian, L. Cheng, A. J. Yin, W. P. Cao, and S. Crichton, “State Detection of Bond Wires in IGBT Modules Using Eddy Current Pulsed Thermography,” *IEEE Trans. Power Electron.*, vol. 29, no. 9, pp. 5000-5009, Sep, 2014.
- [28] Z. Liu, T. Shi, Z. Tang, B. Sun and G. Liao, “Using a low temperature carbon electrode for preparing hole conductor free perovskite hetero junction solar cells under high relative humidity”, *Nanoscale* ,vol.8, no.13, pp.6887–7354, 2016.
- [29] R. Stanway, J. L. Sproston and N. G. Stevens, “Non-linear modeling of an electro-rheological vibration damper”, *J. Eletrast.* , vol.20, no.2, pp.167-84, 1987.

